Nordic Hydrology, 19, 1988, 53-64

Spatial Distribution of Pre-Warm Front Rainfall in the Mediterranean Area

C. Corradini and F. Melone

National Research Council – IRPI, Perugia, Italy

Evidence is given of the distribution of pre-warm front rainfall at the meso-γ scale, together with a discussion of the main mechanisms producing this variability. An inland region in the Mediterranean area is considered. The selected rainfall type is commonly considered the most regular inasmuch as it is usually unaffected by extended convective motions. Despite this, within a storm a large variability in space was observed. For 90 % of measurements, the typical deviations from the area-average total depth ranged from – 40 to 60 % and the storm ensemble-average rainfall rate over an hilly zone was 60 % greater than that in a contiguous low-land zone generally placed upwind. This variability is largely explained in terms of forced uplift of air mass over an envelope type orography. For a few storms smaller orographic effects were found in locations influenced by an orography with higher slopes and elevations. This feature is ascribed to the compact structure of these mountains which probably determines a deflection of air mass in the boundary layer. The importance of this type of analysis in the hydrological practice is also emphasized.

Introduction

It is common knowledge among hydrologists that the large and complex variations in space characterizing precipitation determine considerable difficulties in providing reliable estimations of mean areal rainfall, which is the basic input to rainfall-runoff models (Corradini and Melone 1986). This problem becomes of utmost importance if a dense network of raingauges is not available (Hall and Barclay 1980, Linsley *et al.* 1982). However, a gain in accuracy could be obtained through a

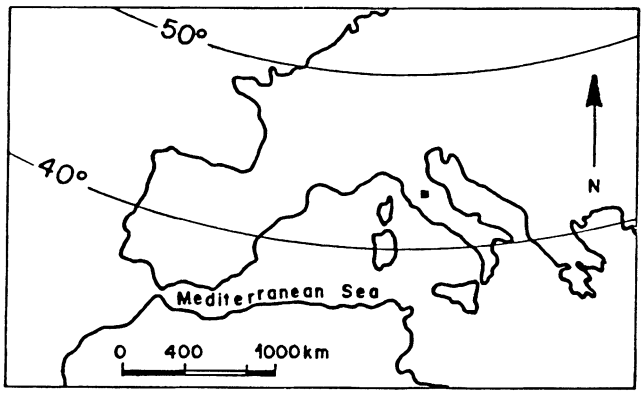

Fig. 1. Location of the study region (■) in the Mediterranean area.

better physical understanding of the causes of natural rainfall variations in space.

It was shown (Browning and Harrold 1969, Harrold and Austin 1974, Parsons and Hobbs 1983) that in mid-latitude frontal systems two important mechanisms contributing to the rainfall spatial variability on the meso-γ scale (see Orlanski 1975) are the forced orographic uplift and convective motions associated with conditions of instability (or potential instability) of air mass. They both occur within areas of large-scale slantwise ascent. All these mechanisms interact in complex fashions with varying degree from storm to storm. It means, for example, that the information on the orographic effects derived from the long-term average distribution of precipitation is of little use in assessing how a particular storm will be influenced by topography. On the other hand for future applications in hydrology, the following synthesis is considered important: (1) the improvement and generalization of understanding for groups of storms produced by frontal systems with similar meteorological characteristics on the large scale and then (2) trying to explain quantitatively the differences in the observed rainfall field from storm to storm through physiographic variables of the basin and local meteorological parameters of easy determination. Despite the development of interesting conceptual models representing frontal systems of different type (Browning 1985), the above problem still is difficult even in the least complex case of pre-warm front rainfall. Valuable investigations on the structure of the rainfall field for the last type of meteorological situation were performed in Britain (Browning *et al.* 1974, Hill and Browning 1979) and in northern USA (Wilson and Atwater 1972, Passarelli and Boehme 1983).

In this paper we will analyse the rainfall spatial distribution associated with mid-latitude pre-warm front meteorological situations over an inland region in Central Italy. The main purpose is to clarify to what extent the results of the aforementioned investigations are representative for a markedly different environment, such as the Mediterranean area. For example, for this area, location shown in Fig. 1, it

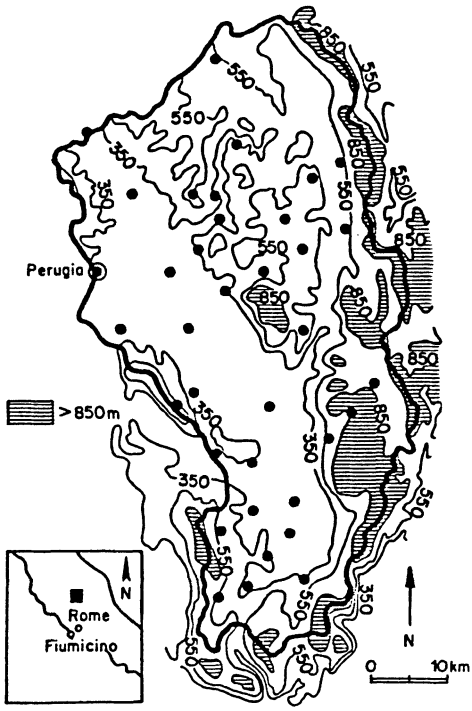

Fig. 2.
Map of the study region with the raingauge positions (•). The 350-, 550- and 850-m contours, partly extending outside the sub-basin boundary (–), are also shown.

may be noted (see Colacino 1983) that (1) except for the southeastern rim, it is surrounded by mountains and hills which induce complicated effects on the large-scale flow; (2) during the cold months the sea surface temperature is generally higher than the air temperature and therefore the Mediterranean Sea provides heat and water vapour to the overlying atmosphere; (3) on the basis of this feature, instabilities and fast evolving weather systems find a favourable environment. Furthermore, we provide here a physical interpretation of rainfall measurements with the objective of deriving useful information for the hydrological practice.

Experimental Area and Raingauge Network

The study region, area 2,282 km^2, is located inside the Upper Tiber River basin. It is shown in Fig. 2 together with the 350,- 550- and 850-m contours. The main features of topography can be synthesized by a large low-land zone with elevation between 200 and 350 m a.s.l. and by a considerable hilly zone in the northern side where a significant percentage of the land ranges in elevation from 350 to 850 m a.s.l. The boundary, except for the northern and northwestern part, is generally characterized by mountains higher than 900 m a.s.l. with peaks ranging in elevation between 1,000 and 1,500 m a.s.l. Figs. 3a and 3b illustrate two profiles provid-

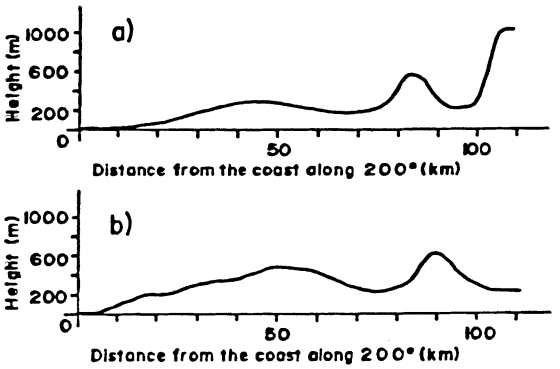

Fig. 3. Cross-sections of the terrain, from the coast to the boundary of the study region, averaged over a 10-km wide strip oriented along 200°: a) Line passing through the southern boundary, b) Line passing close to Perugia.

ing a rough representation of the characteristics of the orography existing between the coast and the boundary of the study region. These two cross-sections, averaged over a 10-km wide strip orientated along 200°, pass through the lower and upper part of the study region, respectively.

The experimental rainfall fields were derived from a raingauge network using 36 instruments whose locations are shown in Fig. 2. The raingauges partly use local recording (29) while the remaining (7) are telemetering raingauges. The network was mainly set up in 1981 by the IRPI, National Research Council of Italy, for the objectives discussed in this paper. It has a larger density in the central zone with northwest-southeast orientation of the hilly terrain and in the southern part of the study region which is bounded to the west by a north-south oriented mountain (see Fig. 2). In a west-east direction this mountain is characterized by the mean orographic slopes of about 15% and -12%, respectively.

Selected Events

Thirteen cyclones that produced widespread precipitation over the study region were considered. The storms analysed here are related to rainfall occurring ahead of surface warm fronts. They were selected according to the following criteria: (1) mean areal precipitation intensity was larger than 0.5 mm/h, (2) precipitation was predominantly in the form of rain because of the problems inherent in obtaining reliable measurements of equivalent snow depth, (3) it was possible, from a surface meteorological analysis, to divide correctly rainfall periods in the pre-warm front phase from those associated with the warm sector passage. A storm was assumed to start when rainfall was observed in anyone of the operating raingauges. The end of

Table 1 –Selected storms and corresponding surface meteorological data.

Storm serial number	Date	Starting time (GMT)	Duration (h)	Air temp. (°C)	Air humidity (%)	Wind speed (km/h)	Wind direction (deg)
1	Feb. 11, 1981	0700	8	8.0	>95	6	180
2	Mar. 2, 1981	1100	5	10.5	>95	6	170
3	Dec. 12, 1981	1900	6	12.0	90-95	7	190
4	Dec. 16, 1981	0500	4	12.0	90-95	10	200
5	Dec. 24, 1981	0600	6	7.5	>95	7	180
6	Mar. 30, 1982	0600	4	9.0	90-95	<2	–
7	Apr. 13, 1982	1900	16	7.0	90-95	10	80
8	Nov. 21, 1983	0700	10	7.0	>95	<2	–
9	Jan. 19, 1984	1300	9	7.0	90-95	7	170
10	Oct. 3, 1984	0900	5	12.5	90-95	8	160
11	Dec. 27, 1984	1700	6	2.5	>95	<2	–
12	Mar. 20, 1985	1600	8	5.5	90-95	11	90
13	Mar. 23, 1985	0700	6	8.0	90-95	15	330

a storm was assumed when the surface warm front passage was observed or when rainfall practically stopped at each gauge. The selected events are summarized in Table 1 together with the values of air temperature, air humidity and speed and direction of wind all averaged throughout the storm duration. These meteorological parameters were derived from measurements in the low-lying flat zone and were used in order to identify the passage of the surface warm front.

As a consequence of the typical distribution of the isobars in the cold season, the development of a cyclone was generally linked with the interaction of the waves of cold and dry air entering the Mediterranean area from NW with the warm and moist air present in this area. Most of the selected cyclones came over the study region from the western Mediterranean area with directions which generally ranged from WSW to NW. Storms 1-6, 8-10, and 13 of Table 1 belong to this class; they were usually characterized by surface wind directions ranging from SSE to SSW. The remaining cyclones came from directions close to south and were associated with surface winds ranging from NE to SE.

Rainfall Field Structure

For each of the 13 storms area-average values of total depth and intensity of rainfall are shown in Table 2. Rainfall intensity was computed for each gauge by dividing the observed total depth (storm depth) by the actual corresponding duration. The considered storm type is characterized by an average storm depth of 9 mm and by a low annual frequency, which indicate its scarce contribution to the total annual

Table 2 – Some characteristics of the storms. The parameter η is linked with the ratio (at each gauge) between the total depth and its area-average value; it represents the range containing 90% of the computed ratios.

Storm serial number	*Area-average rainfall* Duration (h)	Depth (mm)	Intensity (mm/h)	η
1	8	12.4	1.7	0.6-1.5
2	5	5.8	1.4	0.5-1.4
3	6	6.2	1.6	0.7-1.5
4	4	7.9	2.9	0.1-1.7
5	6	6.5	1.3	0.5-1.8
6	4	3.6	1.2	0.5-1.5
7	16	33.2	2.3	0.6-1.7
8	10	7.7	0.8	0.7-1.3
9	9	4.5	0.6	0.4-2.1
10	5	4.3	0.9	0.4-1.7
11	6	6.0	1.3	0.4-1.6
12	8	6.7	1.0	0.5-1.6
13	6	12.5	3.2	0.5-1.6
Ensemble- average	7	9.0	1.6	0.5-1.6

precipitation (of the order of 1,000 mm/year). However, considering the response functions of the Upper Tiber River basin to effective rainfall (Corradini and Singh 1985), the occurrence of these storms over saturated soil may contribute significantly to the development of important flood events with peak flow greater than 500 m^3/s.

For each storm an overall analysis of the spatial variability of rainfall was performed through the estimation, for each gauge, of the ratio between the storm depth and its area-average value. Then, as a rough variability index, the range containing 90% of the computed ratios was adopted. This range, denoted by η and shown in Table 2, is characterized by a little variability throughout the storm ensemble with an ensemble-average of 0.5-1.6 which indicates that a factor three is commonly observed as ratio between largest and smallest storm depths in a given storm. In order to investigate if there exists an organized spatial structure in the rainfall field we analysed the spatial distribution of storm depth both for single storm events and for the fictitious event obtained by averaging the storm depth at each gauge over the storm ensemble. From the single storm event analysis it was found a significant link between topography, represented by an envelope profile with smoothing of isolated peaks and narrow valleys (see also Corradini 1985), and rainfall spatial distribution. However, this link is not of straightforward type. Three sample events are used in order to discuss the main observed features. Fig. 4 shows the observed rainfall field for storm 5. There is a maximum localized over the

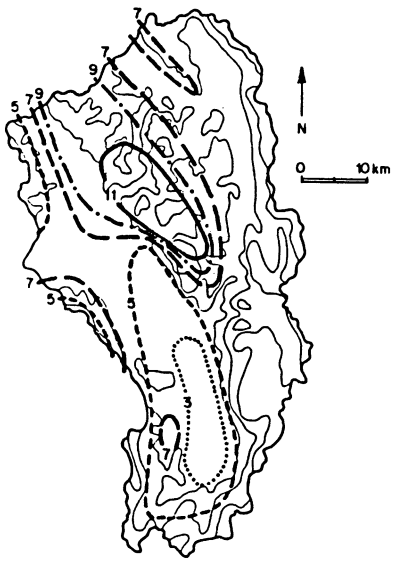

Fig. 4. Observed rainfall field, in mm, for the storm of December 24, 1981. The 350-, 550- and 850-m contours are also shown.

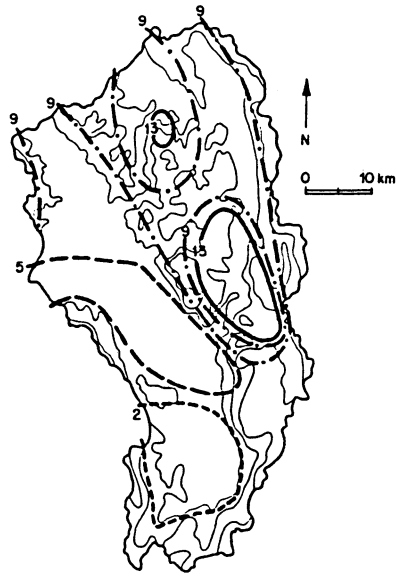

Fig. 5. Observed rainfall field, in mm, for the storm of December 16, 1981. The 350-, 550- and 850-m contours are also shown.

northwest-southeast oriented upslope belt and over a narrow contiguous hilly zone extending ~5 km beyond the hill top of the smoothed orography, a minimum over the low-lying zone located in the southern side of the study region, and a basic value between 5 and 7 mm over the remaining large part of the region. We observe that this part includes in the eastern side the zone over the north-south oriented mountain chain. Fig. 5 shows contours of storm depth for storm 4. The dominant feature, differentiating this case from storm 5, is that here exists a broad area over the hills with values of storm depth ($\geq$9 mm) substantially higher than those observed in the low-lying flat zone ($\leq$5 mm). Furthermore, this area includes smaller zones with still higher storm depths. Fig. 6 illustrates the rainfall spatial distribution for storm 7 which is characterized by the largest values of duration and depth. As it can be seen various features differentiate this storm from the two above described. In this case there is an extended zone with heavier rainfall in the southern side. The zones with lower rainfall are located in the northern and central low-lying area, and in a part of the hilly region rather far from the more significant upslope belts. In order to emphasize the role of effects that are somehow linked to orographic features, a storm ensemble-average spatial distribution of storm depth is shown in Fig. 7. The minimum is computed in the central low-land zone and over the hills far from the main upslope areas, the maximum in the central northwest-southeast oriented upslope belt and in the contiguous zone extending ~4 km, a

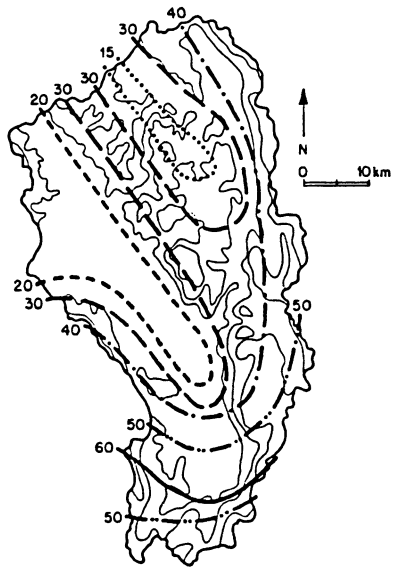

Fig. 6. Observed rainfall field, in mm, for the storm af April 13, 1982. The 350-, 550- and 850-m contours are also shown.

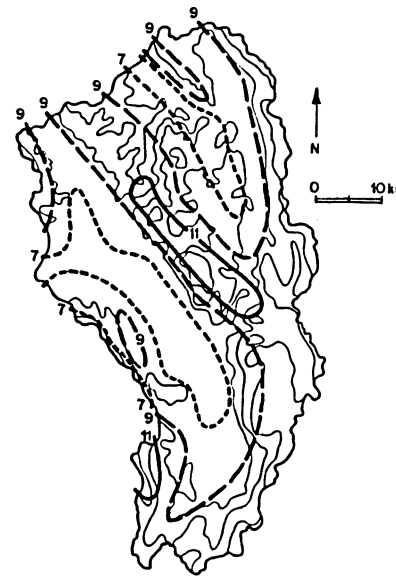

Fig. 7. Storm ensemble-average rainfall field in mm. The 350-, 550- and 850-m contours are also shown.

medium depth was obtained next to the foot of the main upslope areas and in a northwest-southeast oriented belt over the smoothed hills. Considering that the average storm duration was 7 h (see Table 2), the storm ensemble-average rainfall rate over the low-land zone of minimum was 1.0 mm/h while the corresponding value over the close hilly zone of maximum was 1.6 mm/h. The representation in Fig. 7 clearly shows that the average rainfall variability in space is closely related to the main orographic features of the study region. As it was expected (Passarelli and Boehme 1983) the behaviour of the rainfall contours is more regular because the ensemble-average procedure reduces the random contribution produced by non-orographic features to the rainfall variability in space.

Interpretation of Experimental Results

Many studies indicated the seeder-feeder process (Hill *et al.* 1981, Parsons and Hobbs 1983, Passarelli and Boehme 1983) as the main process producing orographic rainfall. Corradini (1985) proposed a diagnostic model incorporating this process together with a representation of the mechanisms of rainfall production directly by forced orographic ascent of evaporation and precipitation drift. Some preliminary applications carried out using an envelope orography over an area (~1,000

km^2) located in the study region considered here showed reasonable model accuracy. We use this model structure as a support in the analysis of the observed rainfall fields, in conjunction with upper air meteorological data observed at Fiumicino (see Fig. 2). Assuming that orographic effects are mainly produced in the lower part of the atmosphere (up to 2,000 m a.s.l.) and dividing this part into layers of equal thickness Δz, the increase in rainfall rate produced in each layer by adiabatic ascent, ΔR_1, and by washout, ΔR_2, may be written in implicit form as

$$\Delta R_1 \equiv F_1 (T, m, \rho, W, a, \Delta z, H) \tag{1}$$

$$\Delta R_2 \equiv F_2 (T, m, \rho, W, a, \Delta z, H, P_i) \tag{2}$$

where

- T – the air temperature,
- m – The mixing ratio,
- ϱ – the air density,
- W – the vertical velocity due to orography,
- a – the height of the layer in the absence of orography,
- H – the height of terrain and
- P_i – the rainfall rate at the level of 2,000 m.

Furthermore, denoting by m_s the saturation mixing ratio and ΔR the total increase in rainfall rate, we have

$$\Delta R \equiv (\Delta R_1 + \Delta R_2) \tag{3}$$

with

$$\Delta R > 0 \quad \text{if} \quad W > 0 \quad \text{and} \quad m = m_s \tag{4}$$

The vertical velocity W is given by

$$W = K(z) \vec{V} \vec{\nabla} H \tag{5}$$

where

- $K(z)$ – a positive coefficient decreasing with the height of the layer,
- $\vec{V}$ – the horizontal wind vector and
- $\vec{\nabla}$H – the local topographic gradient.

Most of the main features of the observed rainfall fields may be easily explained in terms of the above scheme which involves forced uplift of air mass due to orography. For example, the increase (by a factor of about two) observed in the central area of the study region for storm 5 was reasonably well-reproduced. It was determined by the favourable dynamic and termodynamic conditions of the air mass up to 2,000 m. In fact the air was close to saturation before its lifting over the hills, and the average wind speed of ~13 m/s in the range S-SW produced in the upslope belt a scalar product $\vec{V}/\vec{\nabla}H > 0$. It implies, according to Eqs. (4) and (5), $\Delta R > 0$. Futhermore, because of the precipitation drift the increase in precipitation pro-

duced in different layers reached ground both in the upslope belt and in the contiguous downwind zone. This drift process explains the observed broad distribution of the maximum rainfall. In fact the maximum drift $\vec{S}$ may be expressed by

$$\vec{S} = \int_0^{t_m} \vec{V}\, dt \tag{6}$$

where t_M is the maximum time employed by droplets to reach soil surface which may be roughly estimated by

$$t_M = \frac{h_M}{V_f} \tag{7}$$

with h_M maximum height (considered here 2,000 m) and V_f precipitation fall speed. Because the air temperature was greater than 0°C, assuming for V_f the commonly used value of 5 m/s it follows $t_M = 400$ s and, for $\vec{V} = 13$ m/s, the $\vec{S}$ quantity computed along the average downwind direction (~5 km) is comparable with the observed quantity previously given. The same effect was expected to occur in the southwestern side of the study region downwind of the mountains, but it was not observed. This was probably caused by a deflection effect produced by the steep and continuous orographic barrier (see also Fig. 2) which inhibited the forced uplift of the air mass at least in a part of the atmospheric region of thickness lower than the barrier height. The low values of rainfall over the mountains near the eastern boundary were probably due to the same cause. For storm 7, the belt at the foot of the mountain chain near the northeastern boundary was interesting by rainfall values influenced by orographic lifting insofar as below the 1,000-m level easterly winds occurred and the considered belt is located downwind of the chain. In addition the air mass above the 1,000-m level was close to saturation before orographic uplift over the hills and wind direction was from SW. It means that $\Delta R > 0$ in upslope locations and forced orographic uplift contributed to the increase in rainfall depth over the area with northwest-southeast oriented orography. Instead the structure of the rainfall field in the area with heavier precipitation, located in the southern part of the study region, does not seem to be determined by forced uplift, even if a more complex relation with local orography can not be excluded. For storm 4 the upper air data revealed that the air mass was not saturated before orographic uplift over the hills so that evaporation of the rainfall falling from higher atmospheric layers occurred in the entire region between 0 and 2,000 m. On the other hand, over the hills evaporation occurred only in the layer between 1,500 and 2,000 m. Therefore, the large difference in rainfall depth between the extensive area over the hills and the low-land zone was substantially due to the evaporation process. The two regions over the hills with maximum rainfall (see Fig. 5) were probably determined by convective effects triggered by the orographic uplift. This is supported by the upper air data which suggest the probable existence of a layer

potentially unstable around the 1,000-m level. In the southern part of the basin (see Figs. 4 and 5) the existence of meso-γ scale precipitation areas with rainfall depth lower than that observed in the remaining part of the study region may be due to partial evaporation of existing precipitation caused by the descent of air (at least in the higher layers) downwind of the mountains.

Then, the dominant mechanism contributing to increase the rainfall depth at ground may be considered the forced uplift of saturated air due to orography. This produces an orographic cloud which directly or through the interaction with rainfall falling from higher layers provides a precipitation enhancement which is substantially governed by the wind field below the 2,000-m level.

Conclusions

1) Orography, mainly of hilly type, plays an important role in determining the spatial distribution of pre-warm front precipitation in an inland region within the Mediterranean area. In a belt over the hills there was obtained a storm ensemble-average rainfall rate 60% greater than that in the upwind low-land area (1 mm/h). These results are comparable with those observed in a very different environment of the United States (Passarelli and Boehme 1983).

2) A physical interpretation of results, carried out through a parameterized numerical model, indicates that the observed precipitation enhancement was mainly produced by an orographic cloud localized in the lower 2,000 m a.s.l. and that an envelope orography is a suitable representation of terrain in order to explain the main features of rainfall field on the meso-γ scale.

3) A steep and continuous mountain structure, as that existing in the southwestern part of the boundary, may limit the orographic enhancement through the deflection of air mass in a considerable part of the atmospheric region which usually produces the orographic cloud.

4) The results of this study may be usefully employed for practical hydrological purposes. For example, for basins where pre-warm front rainfall plays a dominant role, useful insights for network design and computation of mean areal rainfall may be obtained on the basis of topography and conventional meteorological information.

Acknowledgements

This work was supported by the National Research Council of Italy. The authors wish to thank B. Bani, C. Fastelli and R. Rosi for their assistance in data acquisition.

References

Browning, K.A. (1985) Conceptual models of precipitation systems, *Meteorol. Mag., Vol. 114,* pp. 293-319.

Browning, K.A., and Harrold, T.W. (1969) Air motion and precipitation growth in a wave depression, *Q. J. R. Meteorol. Soc., Vol. 95,* pp. 288-309.

Browning, K.A., Hill, F.F., and Pardoe, C.W. (1974) Structure and mechanism of precipitation and the effect of orography in a wintertime warm sector, *Q. J. R. Meteorol. Soc. Vol. 100,* pp. 309-330.

Colacino, M. (1983) Mediterranean meteorology, Tech. Rep. No. 83/26, IFA National Research Council, Rome, Italy.

Corradini, C. (1985) Analysis of the effects of orography on surface rainfall by a parameterized numerical model, *J. Hydrol., Vol. 77,* pp. 19-30.

Corradini, C., and Singh, V.P. (1985) Effect of spatial variability of effective rainfall on direct runoff by a geomorphologic approach, *J. Hydrol., Vol. 81,* pp. 27-43.

Corradini, C., and Melone, F. (1986) An adaptive model for on-line flood predictions using a piecewise uniformity framework, *J. Hydrol., Vol. 88,* pp. 365-382.

Hall, A.J., and Barclay, P.A. (1980) Design of operational areal rainfall networks using ground-based and radar data, Proc. Int. Symp. on Hydrological Forecasting, Oxford, IAHS Publ. No. 129, pp. 51-56.

Harrold, T.W., and Austin, P.M. (1974) The structure of precipitation systems – A review, *J. Rech. Atmos. Vol 8,* pp. 41-57.

Hill, F.F., and Browning, K.A. (1979) Persistence and orographic modulation of mesoscale precipitation areas in a potentially unstable warm sector, *Q. J. R. Meteorol. Soc., Vol. 105,* pp. 57-70.

Hill, F.F., Browning, K.A., and Bader, M.J. (1981) Radar and raingauge observations of orographic rain over south Wales, *Q. J. R. Meteorol. Soc., Vol. 107,* pp. 643-670.

Linsley, R.K., Kohler, M.A., and Paulhus, J.L.H. (1982) *Hydrology for engineers,* McGraw Hill, New York, pp. 47-96.

Orlanski, I. (1975) A rational subdivision of scales for atmospheric processes, Bull. Am. Meteorol. Soc., Vol. 56, pp. 527-530.

Parsons, D.B., and Hobbs, P.V. (1983) The mesoscale and microscale structure and organization of clouds and precipitation in midlatitude cyclones, IX: Some effects of orography on rainbands, *J Atmos. Sci., Vol. 40,* pp. 1930-1949.

Passarelli, R.E., and Boehme, H. (1983) The orographic modulation of pre-warm-front precipitation in southern New England, *Mon. Weather Rev., Vol. 111,* pp. 1062-1070.

Wilson, J.W., and Atwater, M.A. (1972) Storm rainfall variability over Connecticut, *J. Geophys. Res., Vol. 77,* pp. 3950-3956.

First received: 24 June, 1987
Revised version received: 10 November, 1987

Address:
IRPI/CNR,
Via Madonna Alta 126,
06100 Perugia,
ITALY